ACS APPLIED MATERIALS & INTERFACES

Research Article

www.acsami.org

pH and Thermo Dual-Stimuli-Responsive Drug Carrier Based on Mesoporous Silica Nanoparticles Encapsulated in a Copolymer–Lipid Bilayer

Xin Wu, Zhuyuan Wang,* Dan Zhu, Shenfei Zong, Liping Yang, Yuan Zhong, and Yiping Cui*

Advanced Photonics Center, Southeast University, Nanjing 210096, China

Supporting Information

ABSTRACT: A pH and thermo dual-controllable composite structure was developed as a triggerable drug delivery carrier. In such a drug carrier, a mesoporous silica nanoparticle (MSN) acts as the drug loading core, while a layer of copolymer–lipid serves as the dual-responsive gating shell. Specifically, the copolymer–lipid bilayer consists of natural phospholipids (soy phosphatidylcholine, SPC) and the poly(*N*-isopropylacrylamide-methacrylic acid-octadecyl acrylate) (p(NIPAM-MAA-ODA)) copolymer. With this structure, a high drug loading capacity and a sustained release effect could be provided by the MSN core, while a pH and thermo dual-responsive releasing ability could be offered by the copolymer–lipid bilayer. In addition, the introduction of SPC instead of the traditionally used phospholipids (such as dioleoyl phosphatidylethanolamine (DOPE) or dipalmitoyl phosphatidylcholine (DPPC)) results in a much lower cost and a better serum stability. Using doxorubicin (DOX) as the drug model, our results confirmed that either pH or temperature can trigger the drug release. However, much more drugs could be released by simultaneously controlling the pH and temperature. Furthermore, after being cocultured with cancer cells (MCF-7), the drug carriers transported DOX into the cells and exhibited a pH-sensitive release behavior. Since most tumor sites usually exhibit a more acidic environment or a higher temperature, the pH- and thermo-responsive releasing ability of this drug carrier is particularly useful and important for the targeted release at the tumor region. Thus, due to the powerful controlled releasing ability, the straightforward preparation method, and low cost, the demonstrated nanocarrier will have potential applications in controllable drug delivery and cancer therapy.

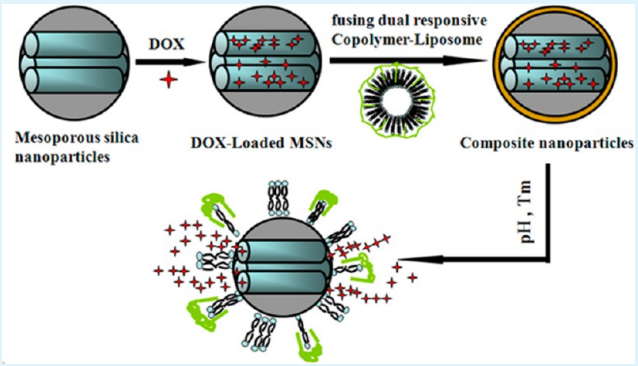

KEYWORDS: *drug carrier, stimuli responsive, mesoporous silica nanoparticles, liposome, copolymer, pH, thermo*

1. INTRODUCTION

In recent years, various nanostructured materials such as mesoporous silica nanoparticles,[1] polymer,[2] and liposome,[3] have been employed as potential drug carriers in the applications of clinical medicine and bioimaging. More recently, a stimuli-responsive drug delivery system has attracted much attention due to its controllable drug release characteristics. Up to now, different external triggers have been successfully demonstrated, such as light,[4] chemical agents (e.g., CdS),[5] pH value,[6] temperature,[7] or magnetic field.[8] Compared with those based on light or chemical agents, pH value and temperature are more attractive stimuli especially suitable for in vivo studies because they do not need extra lasers and will not cause extra damage to human normal tissues.

Considering the fabrication of the drug carriers, the composite structure based on mesoporous silica nanoparticles (MSNs) or liposomes has often been used. As is well-known, MSNs have many advantages, including high surface area and pore volume, high uniformity, tunable pore diameters and surface chemistries, high drug loading capacity, as well as an excellent sustained release effect.[9−11] As another typical drug carrier, liposome has also been widely investigated due to its high biocompatibility with the biomimetic membrane as well as the ease in functionalization.[12] Most recently, a kind of drug carrier based on the integration of MSNs and liposome has been reported.[13,14] By fusing liposome on the surfaces of MSNs, the merits of both MSNs and liposome can be obtained.[15,16] On one hand, because of the mesoporous silica core, the fluxility of the lipid bilayer is suppressed, and the composite nanoparticle can simultaneously load multiple drugs, which significantly improves the drug loading capacity.[16] On the other hand, owing to the good biocompatibility and easy surface functionalization of liposomes,[17,18] it can release drugs in an efficacious and controllable manner. Ashley et al.[19] have reported a nanocarrier by depositing a dioleoyl phosphatidylethanolamine (DOPE) based liposome on mesoporous

Received: July 29, 2013
Accepted: October 15, 2013
Published: October 15, 2013

nanoparticles and observed its pH-dependent release characteristics.[19] Since both the pH value and temperature at the tumor sites are different from those in normal tissues, designing a dual-stimuli-responsive drug carrier will have broad application prospects in clinical applications.[20−28] Recently, some dual-stimuli intelligent systems have been reported.[21−23,25−28] In these nanocarriers, polymeric chains were usually used to act as the controllable switches, such as poly(*N*-isopropylacrylamide-*co*-acrylic acid) (p(NIPAM-*co*-AA)), poly(*N*-isopropylacrylamide-*co*-methacrylic acid) (p(NIPAM-*co*-MAA)), poly(*N*-isopropylacrylamide)-*b*-poly(L-histidine), and so on, while in our proposed drug carriers we focus on the introduction of a shell of lipid bilayer. Compared with the previously existing ones, the fusion process of the lipid bilayer shell is very facile and powerful.

Herein, we demonstrate a simple, efficient, and dual-stimuli-controllable composite structure based on MSNs and copolymer−liposome,[19,29−31] which could release the anticancer drugs upon the stimuli of both pH value and temperature. Since most tumor sites usually exhibit a more acidic environment or a higher temperature, the pH- and thermo-responsive releasing ability of this drug carrier is particularly useful and important for the targeted release at a tumor region. The structure of the composite nanoparticles is demonstrated in Scheme 1. Specifically, a mesoporous silica nanoparticle acts as the drug loading core, and the copolymer−liposome serves as the gating shell. The copolymer−liposome consists of natural phospholipids (soy phosphatidylcholine, SPC) and p(NIPAM-MAA-ODA) copolymer, in which *N*-isopropylacrylamide (NIPAM) of the copolymer takes the role of thermo-sensitive materials[32,33] while methacrylic acid (MAA) acts as pH-sensitive molecules.[34−36] As reported by Ashley et al., natural phospholipid SPC was less expensive than the typical synthetic phospholipids of DOPE and dipalmitoyl phosphatidylcholine (DPPC).[19] More importantly, many previous reports have demonstrated that the liposome composed of DOPE showed a relatively poor stability in serum.[31,37−39] So the presented method using copolymer−liposome could solve the problem of instability while retaining the pH and thermo sensitivity.[40−44] Furthermore, the release behavior of this system under conditions of different temperature and pH value was investigated using a classic anticancer drug, doxorubicin hydrochloride (DOX), as the model.[45] Finally, the cellular uptake of this drug carrier in MCF-7 cells and the pH-dependent release behaviors were investigated as well as their cytotoxicity.

Scheme 1. Schematic Illustration of the Dual-Responsive Drug Carrier Based on Mesoporous Silica Nanoparticles Encapsulated in a Copolymer−Lipid Bilayer

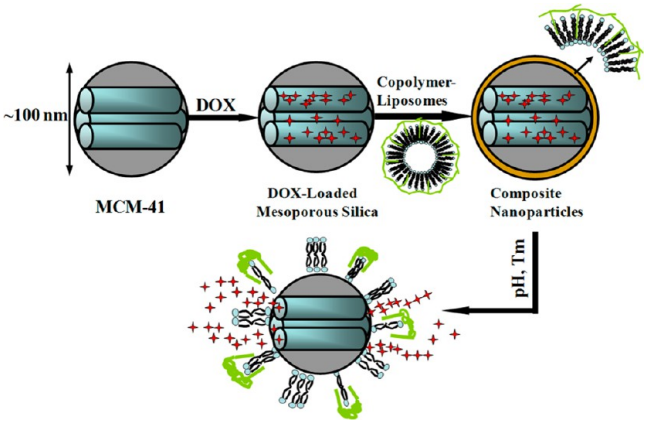

2. EXPERIMENTAL SECTION

2.1. Materials. *N*-Isopropylacrylamide (NIPAM), methacrylic acid (MAA), azobisisobutyronitrile (AIBN), 1,4-dioxane, and doxorubicin hydrochloride (DOX) were purchased from Aladdin Industrial Corporation. Octadecyl acrylate (ODA) was purchased from Sigma. Diethyl ether and tetrahydrofuran were purchased from Sinopharm Chemical Reagent Co., Ltd. Soya bean lecithin (SPC, purity 97%), cholesterol, cetyltrimethylammonium bromide (CTAB), tetraethylorthosilicate (TEOS), and (3-aminopropy)trimethoxysilane (APTMS) were purchased from Alfa Aesar. Sodium hydroxide (NaOH) was purchased from Guangdong Xilong Chemical Co., Ltd. Hydrochloric acid (HCl) was purchased from Shanghai Chemical Reagent Co., Ltd. Ethanol was purchased from Nanjing Chemical Reagent Co., Ltd. Chloroform and methanol were purchased from Shanghai Lingfeng Chemical Reagent Co., Ltd. Phosphate-buffered saline (PBS, pH 7.4) was purchased from Nanjing Bookman Biotechnology Co., Ltd. Deionized water with a resistivity of 18.2 MΩ/cm was used in all the above experiments.

2.2. Synthesis of Dual-Controllable Copolymer−Liposome. The copolymer p(NIPAM-MAA-ODA) was synthesized by the previously reported method.[31,46] Typically, monomers containing 3 g of NIPAM, 0.5768 g of MAA, and 0.1136 g of ODA (molar ratio 76:19:1) were dissolved in 20 mL of 1,4-dioxane. Then the initiator 0.068 g of AIBN was added to the solution. The mixture was degassed through bubbling N_2 for 15 min and then reacted at 70 °C for 14 h. The mixture was precipitated in diethyl ether. The precipitation was redissolved in tetrahydrofuran and reprecipitated with diethyl ether three times. Finally, the product was dried for use.

Then, the copolymer−liposome was synthesized by the membrane evaporation method.[47] In the experiments, 90 mg of SPC and 10 mg of cholesterol were dissolved in a 10 mL mixture of chloroform and methanol (v/v = 4:1). Then, 30 mg of the as-prepared copolymer (30 wt %) was added. The mixture was evaporated at 40 °C for 4 h by a rotatory evaporator and then hydrated with PBS solution for 2 h. Then, the copolymer−liposome solution was obtained and stored at 4 °C. The concentration of the copolymer−liposome was about 10 mg/mL.

In a control experiment, the liposome composed of DOPE/OA was synthesized by the same membrane evaporation method.[47] DOPE and OA (molar ratio 6:4) were dissolved in a 10 mL mixture of chloroform and methanol (v/v = 4:1). The procedures of evaporation and hydration were the same as that of copolymer−liposome synthesis.

2.3. Synthesis of Copolymer−Lipid Bilayer Coated MSNs. MSNs were synthesized using a conventional procedure.[1] Amounts of 1 g of CTAB and 0.28 g of NaOH were dissolved into 480 mL of deionized water and stirred at 80 °C. After the solution became clear, 5 mL of TEOS was added dropwise within 20 min. The stirring was continued for at least 4 h. Then the milk-white mixture was collected by centrifugation at 6500 rpm for 10 min. To remove the CTAB surfactant, the prepared materials were washed several times with a mixture of ethanol and diluted hydrochloric acid. Finally, the products were redissolved in 10 mL of ethanol.

Then, the surfaces of MSNs were modified with APTMS, and the product was denoted as MSN-NH_2. In a typical experiment, 300 μL of APTMS was added into 10 mL of the as-prepared MSNs in ethanol and stirred overnight. The mixture was centrifuged and washed with ethanol and water at least 3 times. The products were redispersed in 0.5 × PBS.

Finally, the copolymer-liposome (2.5 mg/mL) was added into the as-prepared MSN-NH_2 (v/v=4:1).[13,14,16,19,29] The mixture was allowed to stand at room temperature for 1 h.[29,30] Extra copolymer-liposome and the supernatant were removed by centrifugation at 5000 rpm for 5 min. The nanocomposites (denoted as MSN-NH_2@colipid) were subsequently washed with 0.5 × PBS for three times and finally dispersed in PBS solution.

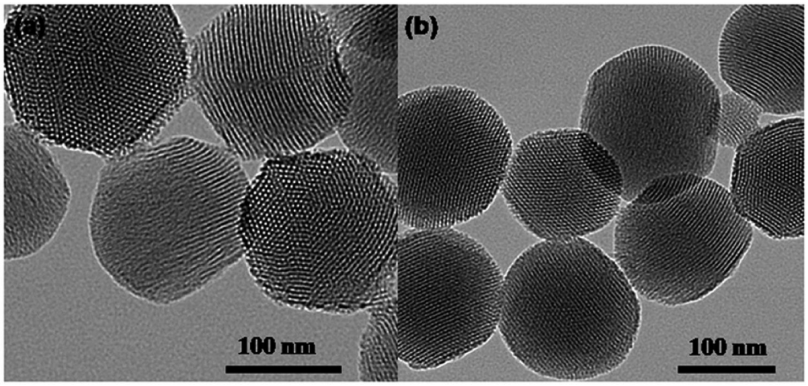

Figure 1. TEM images of (a) MSNs and (b) MSN-NH_2 nanoparticles.

2.4. In Vitro Drug Loading and Release. An amount of 2 mL of MSN-NH_2 solution was washed three times with deionized water. The precipitate was diluted with 3 mL of deionized water. Then, 200 μL of DOX (5 mg/mL) was added. After incubating the above mixture for 8 h in the dark, MSNs loaded with doxorubicin (denoted as DOX@MSN-NH_2) were collected by centrifugation at 6500 rpm for 15 min. Then the copolymer−liposome was fused onto the surfaces of DOX@MSN-NH_2 (denoted as DOX@MSN-NH_2@colipid). To investigate the pH-dependent releasing efficiency, three aliquots of the composite nanoparticles with equal amount were immersed in 3 mL of buffer solution at 25 °C with pH = 7.4, pH = 6.8, and pH = 5.5, respectively. The mixture was shaken at certain time intervals. The supernatant was taken out by centrifugation to measure the absorption, and an equal volume of fresh medium was added instead. By comparing the absorption curve of pure DOX in different pH solutions,[48] the amount of released DOX can be calculated.

To investigate the thermocontrollable release efficiency of this drug carrier, three sets of DOX@MSN-NH_2@colipids with equal amount were immersed in 3 mL of PBS buffer (pH = 7.4) at T = 25 °C, T = 42 °C, and T = 45 °C. The procedure of absorption measurement was the same as that of a pH-dependent release investigation.

Finally, to study the release efficiency upon dual stimulation as pH and temperature, four aliquots of DOX@MSN-NH_2@colipid with equal amounts were immersed under four different conditions, which were pH = 7.4 at T = 37 °C, pH = 7.4 at T = 42 °C, pH = 5.5 at T = 37 °C, and pH = 5.5 at T = 42 °C, respectively. The procedure of absorption measurement was the same as above.

2.5. Cell Culture Experiment. MCF-7 cells were purchased from China Type Culture Collection and cultured in DMEM under standard cell culture conditions (5% CO_2, 37 °C). Media were supplemented with 10% fetal bovine serum (Gibco) and 1% penicillin−streptomycin (Nanjing KeyGen Biotech. Co., Ltd.).

To investigate the drug delivery behavior of the composite nanoparticles in vitro, MCF-7 cells were seeded into a culture dish and incubated for 24 h. Subsequently, 50 μL of the prepared DOX@MSN-NH_2@colipid solution was added into the culture dish (volume ratio nanocarriers solution:culture media = 1:50) and incubated for 3 h. To observe the intracellular releasing effects, the culture media containing excess nanocarriers were discarded and replaced by 2 mL of pH = 7.4 and pH = 5.5 buffer solution. The cells were further incubated for 30 min and 1 h, respectively. Before the fluorescence measurement, the buffer solutions were discarded, and the culture dishes were washed twice with PBS.

2.6. Cell Viability Assays. The cell viability of MCF-7 cells incubated MSN-NH_2@colipid was investigated by 3-(4,5-dimethylthiazol-2-yl)-2,5-diphenyltetrazolium bromide (MTT) assays (Nanjing KeyGen Biotech. Co., Ltd.). MCF-7 cells were seeded in 96-well plates with a density of 1 × 10^4 cells/mL and cultured for 24 h at 37 °C under a 5% CO_2 atmosphere. Then, 2.5, 5, 7.5, and 10 μL of MSN-NH_2@colipid nanocarrier solution were added into the culture media of MCF-7 cells for 36 h. After that, 50 μL of MTT solution (MTT buffer to dilution buffer 1:4) was added into each well, and the plates were incubated for another 4 h. The reaction was terminated by adding 150 μL of DMSO after removing the supernatant medium. When the purple formazan crystals were resolved by DMSO, the absorbance of the wells at 490 nm was measured with a microplate reader (Bio-Rad model 680). Cells incubated in the absence of nanocarriers were used as a control.

2.7. Instrumentation for Measurements. Transmission electron microscope (TEM) images were obtained with a Tecnai G^2T20 transmission electron microscope operating at 200 kV. The TEM image of the copolymer−liposome was obtained by staining them with 1.5% phosphotungstic acid. The absorption spectra were recorded on a Shimadzu UV-3600 PC spectrophotometer with quartz cuvettes of 1 cm optical path length. Fluorescence was measured by a FLS920 Fluorescence spectrometer (Edinburgh). Intracellular fluorescence images were measured by an Olympus FV 1000 confocal system with an excitation at 488 nm.

3. RESULTS AND DISCUSSION

3.1. Characterization of MSN-NH_2. In recent years, MSNs have become one of the potential drug carriers due to their ordered porous structures, high loading capacity, and low cytotoxicity. In our presented drug carrier, MSNs are chosen as the core to achieve a large loading amount. The TEM images of MSNs and MSN-NH_2 are shown in Figure 1a and 1b, respectively. Figure 1a shows that the prepared MSNs have a uniform spherical shape with an average diameter of about 100 ± 10 nm. Moreover, the porous structure of MSNs can be clearly observed, which consists of a series of parallel channels with a hexagonal geometry. Comparing Figure 1a and 1b, it can be found that the modification of amino groups did not change the morphology of the MSNs. However, it reversed the surface charge of MSNs. Our experimental results showed that the surface potential of the original MSNs was −25 mV, while that of the MSN-NH_2 was +35 mV. Besides, the Fourier-transform IR (FTIR) spectra of bare MSN and MSN-NH_2 nanoparticles are also obtained and shown in Figure S1 (Supporting Information, SI). The unmodified MSNs show the typical vibration bands of siliceous materials, such as that of asymmetric stretching Si−O−Si at 1085 cm^{-1}, symmetric stretching Si−O−Si at 800 cm^{-1}, and stretching vibrations of Si−OH groups at 960 cm^{-1}.[49] However, after the modification of amino groups, the emergence of a new peak at 1560 cm^{-1} is attributed to the scissor vibration peak of NH_2. The bands at 3300−3400 cm^{-1} and 2934 cm^{-1} appear, which belong to the stretching vibration of N−H and C−H bonds.[50−52] This suggests that the amino groups were successfully grafted onto the surfaces of mesoporous silica nanoparticles.

3.2. Characterization of the Copolymer−Liposome. In our presented drug carrier, the pH- and thermo-stimuli responsive ability is provided by the p(NIPAM-MAA-ODA) copolymer, which is further incorporated with liposome to serve as the shell. Thus, in our first step, the copolymer−liposome was prepared according to the previously reported methods,[12,31] whose morphology is shown in Figure 2a. It can

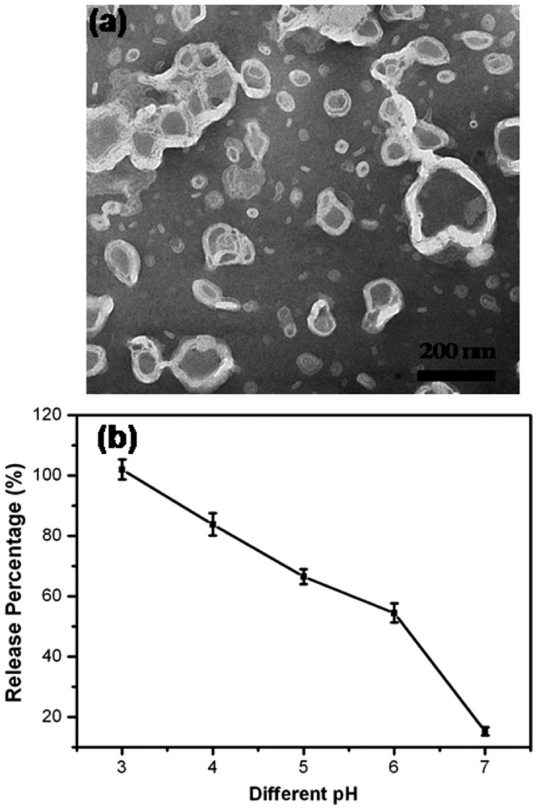

Figure 2. (a) TEM images of copolymer−liposome and (b) pH-sensitive release percentage of calcein from the copolymer−liposome. For TEM imaging, the copolymer−liposome was stained with 1.5% phosphotungstic acid.

be found that after being incorporated with copolymer the copolymer−liposome could still maintain a liposome-like shape. Further, to investigate the pH-dependent drug release characteristics, calcein was loaded in the copolymer−liposome. By measuring the fluorescence of calcein released from the copolymer−liposome, the percentage of released calcein under different pH values was obtained, as shown in Figure 2b. When loaded inside the copolymer−liposome, the fluorescence of calcein was not observable due to the high concentration-induced self-quenching. However, the fluorescence was recovered by disrupting the copolymer−liposome bilayer with Triton X-100. From Figure 2b, it can be observed that the releasing amount of calcein increases at lower pH value. Specifically, the release percentage at pH 7.0 was 20%, which increased to about 63% at pH 5.0 and nearly 100% at pH 3.0. In addition, to obtain the phase transition temperature (T_m) of the copolymer−liposome, the lower critical solution temperature (LCST) was also measured under pH 5.5 and pH 7.4, respectively. The plotted curves were shown in Figure 3, which indicate that the T_m at pH = 5.5 and pH = 7.4 are 37 and 42 °C, respectively.

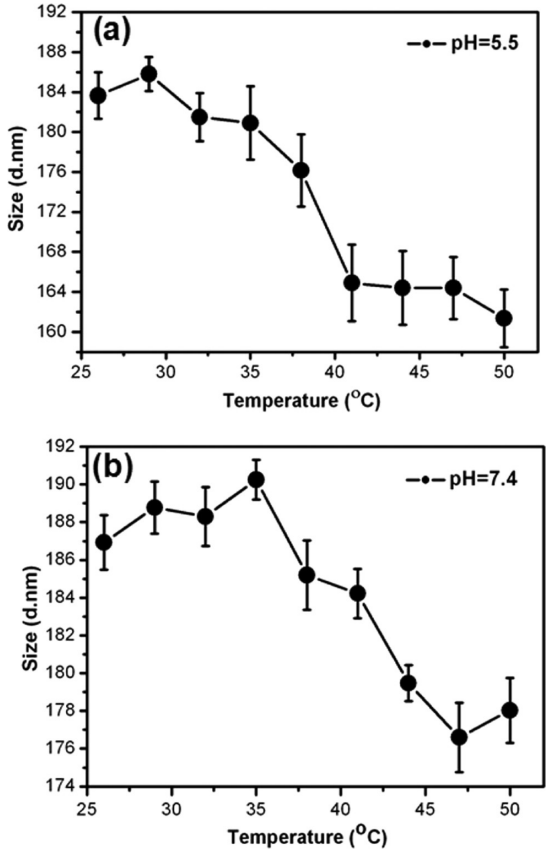

Figure 3. Hydrodynamic diameter measurements of the copolymer−liposome as a function of temperature in different pH buffer solutions: (a) pH = 5.5 and (b) pH = 7.4.

As previously reported by many groups, the liposome composed of DOPE showed a relatively poor stability in serum.[31,37−39] Thus, to investigate the serum stability of the copolymer−liposome used in our experiments over DOPE, the calcein-releasing experiments in serum and PBS solution were performed for comparison. The results were shown in Figure S4 (SI). As shown in the figure, in PBS buffer solution, the releasing amount of calcein after 20 h is similar to the DOPE/OA liposome and copolymer−liposome (SPC). However, in serum, the releasing amount of calcein from DOPE liposome is much more than that from copolymer−liposome (SPC) within 20 h. These results indicate that the serum stability of copolymer−liposome (SPC) is indeed better than that of DOPE/OA liposome, which was in agreement with the results reported by other groups.[31,37−39]

3.3. Characterization of the Composite MSN-NH_2@colipid. The as-prepared copolymer−liposome was fused on the surfaces of MSN-NH_2 to form the MSN-NH_2@colipid nanocomposite, whose TEM image is shown in Figure 4a. Comparing Figure 4a with Figure 1b, it could be observed that the surfaces of MSN-NH_2@colipid nanoparticles are much rougher than those without the colipid layer, and the porous structure is not as clear as before. Besides, the surface charge of the MSN-NH_2@colipid is about −32 mV, while that of the MSN-NH_2 is +35 mV. Furthermore, to confirm the formation of such composite structures more vigorously, the membrane of the phospholipid layer was ruptured by alcohol,[53] and the TEM image of the resultant MSNs is shown in Figure 4b. As can be observed, the porous structure of MSNs was perfectly retained,

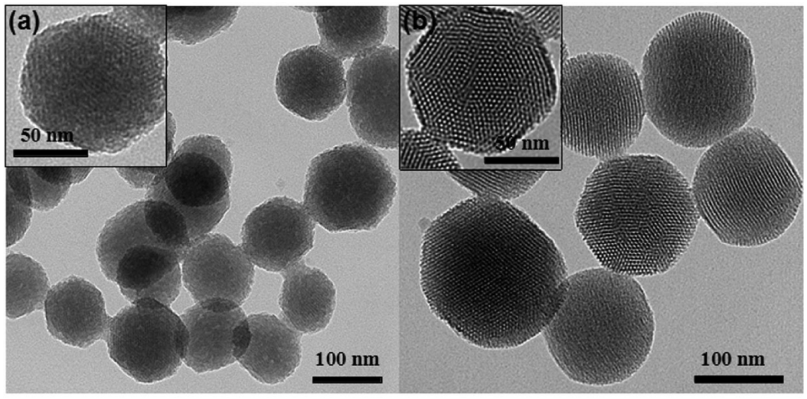

Figure 4. TEM images of (a) MSN-NH_2@colipid nanoparticles and (b) the composite nanoparticles with the phospholipid layers being ruptured by alcohol.

which means that the coating of the copolymer–lipid bilayer did not influence the structure of MSNs. On the other hand, this result also proves that the copolymer–lipid bilayer was coated on the MSNs.

Further, to obtain more evidence of the successful coating of the copolymer–lipid bilayer, the rupturing experiment of the copolymer–lipid bilayer was also conducted using calcein as a model. In the experiment, calcein was first loaded into the MSNs, followed by fusing the lipid bilayer on the MSNs. Then alcohol was added to destroy the lipid bilayer. The mixture was centrifuged, and the absorption and fluorescence of calcein in the supernatant were measured. Calcein-loaded MSN-NH_2@colipid without the addition of alcohol was used as the control and subjected to the same centrifugation and measurment procedures. The results are shown in Figure 5a and 5b, respectively. As can be seen, the addition of alcohol resulted in stronger absorption and fluorescence of calcein, which is due to the destruction of the lipid bilayer shell and subsequent release of calcein. All the above results indicate that the copolymer–liposome was successfully fused onto the surfaces of MSN-NH_2.

3.4. Drug Release Behavior of DOX@MSN-NH_2@colipid. The pH- and thermo-responsive drug release behavior of our presented drug carrier was investigated using DOX as the model drug, which was preloaded into MSN-NH_2 as described in the Experimental Section. According to the calculation method[54−56] and our experimental parameters, the encapsulation efficiency of MSN-NH_2 for DOX was about 47.8% when incubating DOX with MSN-NH_2 for 8−10 h, and the absolute drug loading content was about 29.51 μg/mg. The detailed calculation method was given in the Supporting Information.

To investigate the pH-dependent releasing characteristics, three different pH values (pH 7.4, pH 6.8, and pH 5.5) were selected, which simulate the pH value of blood, tumor extracellular region, and endosomes.[50] Then, the release process of the DOX@MSN-NH_2@colipid under the above three pH conditions was monitored at certain time intervals within 24 h at 25 °C. As shown in Figure 6a, the amounts of released DOX increased with reduced pH value. Specifically, about 11% of DOX was released at pH = 7.4, while about 19% of DOX was released at pH = 6.8 in 23 h. However, at pH = 5.5, the released amount of DOX significantly increased to about 46%, more than four times that at pH = 7.4. This is because MAA molecules of the copolymer–lipid bilayer exhibit an extended hydrophilic state under neutral pH conditions,

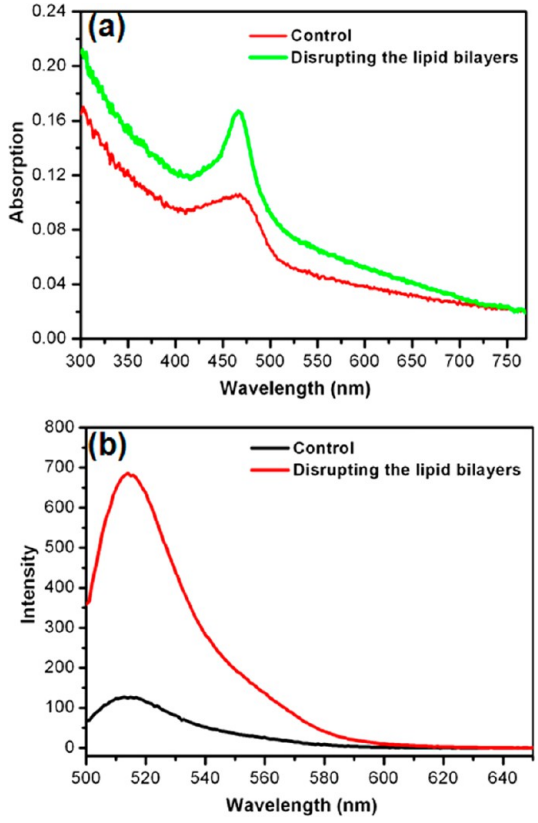

Figure 5. Absorption (a) and fluorescence (b) spectra of calcein in the supernatant before and after the addition of alcohol.

which changes to a hydrophobic spherical structure after acidification. Such a conformational change rearranges the phospholipid bilayer and alters its barrier property. For comparison, the release curve of DOX@MSN-NH_2 was also obtained as a control, and the results are depicted in Figure 6b. The release efficiency was 45%, 53%, and 69% corresponding to pH 7.4, pH 6.8, and pH 5.5, respectively. Thus, the difference in the amount of released DOX between the three pH values was not as obvious as that of the DOX@MSN-NH_2@colipid. Consequently, the prepared composite drug carrier exhibited a more pronounced pH-controllable property than that without the copolymer–liposome layer. This is very important in practical applications of pH-responsive drug carriers because of

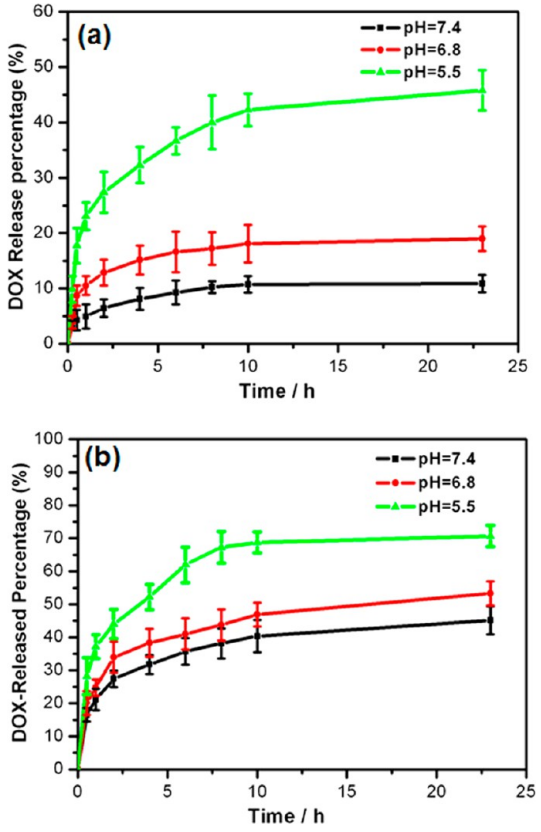

Figure 6. pH-responsive release curves of DOX@MSN-NH_2@colipid nanoparticles (a) and DOX@MSN-NH_2 (b) under pH 5.5, 6.8, and 7.4 at 25 °C.

the more acidic environment of tumor tissues than that of the normal ones.

Moreover, to exclude the possibility that the transport efficiency of DOX itself may vary with pH values, another drug model of 9-aminoacridine hydrochloride monohydrate (9AA) was used to check the universality of our nanocarrior. The release performance under different pH conditions was shown in Figure S2 (SI). As shown in the figure, similar drug release characteristics were observed. The release efficiency was about 48.1% at pH 5.5, about twice that at pH 7.4. Thus, it was reasonable to conclude that the pH sensitivity of our proposed nanocarrier system was not dependent on the chosen test drug.

Once the pH-controllable release characteristics were confirmed, the thermo-dependent release performance was investigated. As shown in Figure 3b, at pH 7.4, the phase transition temperature (T_m) of copolymer–liposome is around 42 °C. Thus, in our experiments, the release curves at three different temperatures (25 °C ($T < T_m$), 42 °C ($T = T_m$), and 45 °C ($T > T_m$)) were obtained with pH value fixed at 7.4. The experimental results are shown in Figure 7. The releasing efficiency of DOX at 42 °C (T_m) reached 54% after 22 h, which is significantly higher than those at the other two temperatures (31% at 45 °C and 15% at 25 °C). This is consistent with the property of the copolymer–liposome as reported by the previous literatures.[31] The reason could be explained as follows. Briefly, when the temperature is below T_m, the loaded drugs are leaked through the diffusion process. However, when the temperature reaches the T_m value of the copolymer–lipid bilayer, the hydrophobic tails of phospholipid are in the perpendicular states, which means the "door" is open at a

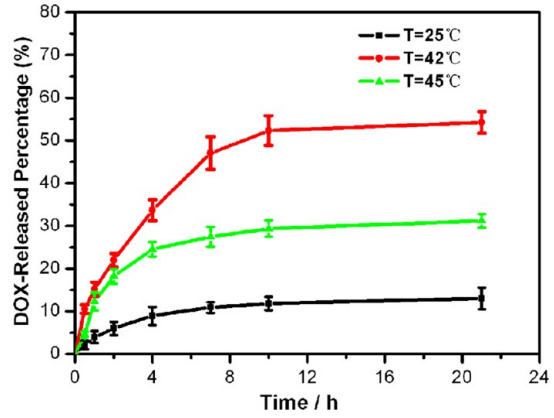

Figure 7. Thermo-responsive release curve of DOX from the nanocomposite at pH = 7.4.

maximum extent and most drugs can be released. When the temperature increases to be higher than T_m, the hydrophobic tails of phospholipids become parallel to the surfaces, which hampers the release of drugs from the MSN core. The above results indicate that the drug carrier indeed holds a thermo-responsive releasing ability.

Furthermore, we investigated the dual triggered releasing property of this drug carrier using both pH value and temperature as the stimuli. Since the T_m of this copolymer–liposome is about 37 °C at pH = 5.5 and 42 °C at pH = 7.4 (Figure 3), four sets of pH and temperature conditions were selected for comparison, which are (1) pH = 7.4 and T = 37 °C, (2) pH = 7.4 and T = 42 °C, (3) pH = 5.5 and T = 37 °C, and (4) pH = 5.5 and T = 42 °C. Since tumor regions generally exhibit a more acidic environment[57] or a higher temperature[21] than the normal ones, the first set of conditions could simulate that of normal tissues, while the latter three sets could simulate those of tumor sites. Figure 8 shows the release curves of DOX

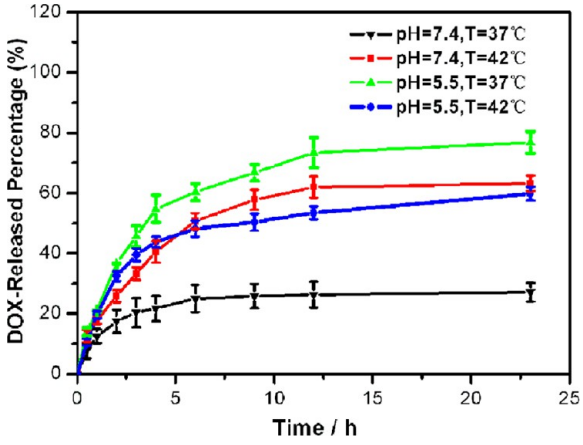

Figure 8. Dual-controllable release curve of DOX from the prepared composite nanoparticles.

under the above four different conditions. As shown in the figure, after an incubation time of 24 h, the releasing efficacy of DOX is largest (76.8%) under the lowest pH value and its corresponding T_m (pH 5.5 and T = 37 °C). However, for pH value = 7.4, the releasing efficacy decreased to only about 27% even at the same temperature (37 °C). This is because 37 °C is lower than the corresponding T_m at pH 7.4. Simiarly, the releasing amount (pH 5.5 and T = 42 °C) was less than that of

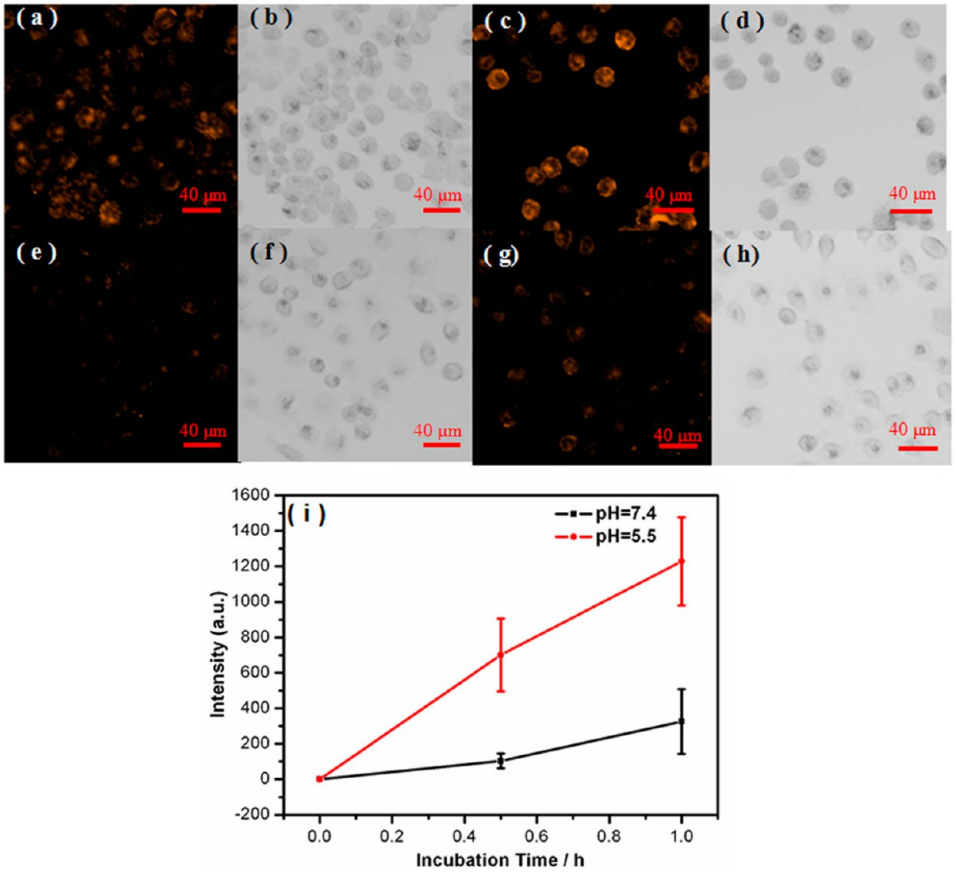

Figure 9. Fluorescence and bright-field images of MCF-7 cells incubated with the DOX@MSN-NH_2@colipid at pH 5.5 for 30 min (a,b) and 1 h (c,d) and at pH 7.4 for 30 min (e,f) and 1 h (g,h). Average fluorescence intensities of a single MCF-7 cell incubated with the nanocarriers at pH = 7.4 and 5.5 for 30 min and 1 h, respectively. The error bars represent the standard deviation of 18 measurements (i).

pH 5.5 and T = 37 °C. It was because that 42 °C was not the T_m at pH = 5.5. So, it is reasonable that the releasing efficacy increased to 60% under the conditions of pH 7.4 at 42 °C because 42 °C is the corresponding T_m of pH 7.4. Thus, all the above results indicate that the drug release can be controlled by tuning both pH value and temperature. More importantly, this result demonstrated that our presented drug carrier could release much more drugs at tumor sites than normal tissues with either a more acidic condition or a higher temperature. Thus, this kind of pH- and thermo-stimuli responsive drug carrier holds great potential in the applications of controllable drug delivery and cancer therapy.

3.5. Intracellular pH-Responsive Drug Delivery. First, an extra experiment was performed to prove that the nanocarriers can enter the living cells. In the experiments, the MSNs were first covalently grafted with rhodamine isothiocyanate (RhBITC) to yield fluorescence and subsequently fused with the copolymer–liposome shell. Then, a series of fluorescence images at different depths within the cells were taken with an interval of 1 μm using a confocal laser scanning microscope with a 60 × object to keep a longitudinal resolution better than 1 μm. The results were shown in Figure S3 (SI), where the position of the culture dish surface was set to 0 μm. Obviously, no fluorescence was obtained beyond the locations of the cells, while strong fluorescent images were observed within the cells. Moreover, it can be found that the nanocarriers were mainly distributed in the cytoplasmic region. Since RhBITC was covalently doped inside the nanocarriers, the fluorescence could only originate from the nanocarriers. Thus, it is reasonable to conclude that the nanocarriers were located inside the living MCF-7 cells.

Then, to investigate the in vitro pH-responsive release behavior of the drug carrier, MCF-7 cells were used as the model cancer cells, and the procedure was depicted in the Experimental Section. The intracellular fluorescence images of DOX at pH values of 5.5 and 7.4 are shown in Figure 9(a–h). Obviously, the fluorescence intensity in cells under pH 5.5 is stronger than that under pH 7.4 at the same incubation time, and the fluorescence intensity with an incubation time of 1 h was stronger than that of 30 min under the same pH conditions. Besides, the average fluorescence intensities of a single cell were shown in Figure 9(i) for a clearer comparison. These results provide direct evidence for the pH-sensitive releasing behavior of DOX@MSN-NH_2@colipid nanoparticles.

Finally, the MTT assay was performed to examine the cytotoxicity of this presented drug carrier. As shown in Figure 10, MSN-NH_2@colipid nanoparticles exhibit no obvious cytotoxicity to the cells and have a good biocompatibility. Considering that the ultimate goal of such nanocarriers is to load cancer drugs to implement the controlled intracellular drug delivery and to avoid side effects caused by a universal cytotoxicity, this kind of new material holds great potential in clinical application.

4. CONCLUSIONS

In summary, using NIPAM-MAA-ODA copolymer–liposome and MSNs, a pH and thermo dual-responsive drug carrier was

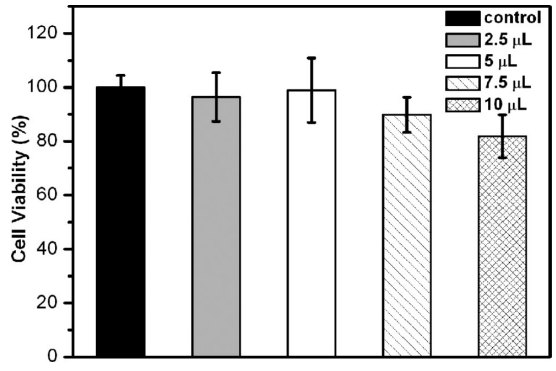

Figure 10. Viability of MCF-7 cells incubated with MSN-NH_2@colipid. MCF-7 cells incubated with standard culture media were used as control.

demonstrated. Due to the dual-sensitive copolymer−liposome, the releasing efficiency of DOX can be controlled by both pH and temperature. Under sole pH stimulation, the maximum releasing amount was about 46% at pH = 5.5, nearly four times that at pH 7.4, and when temperature was used as the only stimulus, the maximum releasing amount was approximately 54% at T = 42 °C under pH = 7.4, about five times that at T = 25 °C. However, under simultaneous pH and temperature triggering, the accumulative release of the composite structure showed a low premature leakage (only 27%) at pH = 7.4, T = 37 °C, while the release efficacy significantly increased to 76.8% at pH = 5.5, T = 37 °C. The results confirmed that both pH and temperature could be employed as the switches. Since tumor sites usually exhibit a more acidic environment or a higher temperature, the releasing results under different combinations of pH and temperature conditions show that more drugs could be released under a tumor-like region than a normal one. Thus, a simple, highly effective, and dual-responsive nanocomposite has been demonstrated, which is a promising anticancer drug carrier for clinical applicaitions.

■ ASSOCIATED CONTENT

Ⓢ Supporting Information

Figures S1−S4 and calculation of drug loading content (LC) and encapsulation efficiency (EE). This material is available free of charge via the Internet at http://pubs.acs.org.

■ AUTHOR INFORMATION

Corresponding Authors

*E-mail: wangzy@seu.edu.cn.
*E-mail: cyp@seu.edu.cn.

Notes

The authors declare no competing financial interest.

■ ACKNOWLEDGMENTS

This work was supported by the Natural Science Foundation of China (NSFC) (Nos. 61275182, 61177033, 21104009), Science Foundation for The Excellent Youth Scholars of Southeast University, the Scientific Research Foundation of Graduate School of Southeast University (YBJJ1125), the Scientific Innovation Research Foundation of College Graduate in Jiangsu Province (CXZZ12_0094), and the Fundamental Research Funds for the Central Universities.

■ REFERENCES

(1) Lu, Y. F.; Fan, H. Y.; Stump, A.; Ward, T. L.; Rieker, T.; Brinker, C. J. *Nature* **1999**, *398*, 223−226.
(2) Morones, J. R.; Frey, W. *Langmuir* **2007**, *23*, 8180−8186.
(3) Ishihara, A.; Yamauchi, M.; Tsuchiya, T.; Mimura, Y.; Tomoda, Y.; Katagiri, A.; Kamiya, M.; Nemoto, H.; Suzawa, T.; Yamasaki, M. *J. Biomater. Sci., Polym. Ed.* **2012**, *23*, 2055−2068.
(4) Vivero-Escoto, J. L.; Slowing, I. I.; Wu, C. W.; Lin, V. S. Y. *J. Am. Chem. Soc.* **2009**, *131*, 3462−3463.
(5) Kim, M. J.; Lee, H. J.; Lee, I. A.; Kim, I. Y.; Lim, S. K.; Cho, H. A.; Kim, J. S. *Arch. Pharmacal Res.* **2008**, *31*, 539−546.
(6) Ishida, T.; Okada, Y.; Kobayashi, T.; Kiwada, H. *Int. J. Pharm.* **2006**, *309*, 94−100.
(7) Kono, K.; Murakami, T.; Yoshida, T.; Haba, Y.; Kanaoka, S.; Takagishi, T.; Aoshima, S. *Bioconjugate Chem.* **2005**, *16*, 1367−1374.
(8) Baeza, A.; Guisasola, E.; Ruiz-Hernandez, E.; Vallet-Regi, M. *Chem. Mater.* **2012**, *24*, 517−524.
(9) Gu, J.; Fan, W.; Shimojima, A.; Okubo, T. *Small* **2007**, *3*, 1740−1744.
(10) Vallet-Regi, M.; Ramila, A.; del Real, R. P.; Perez-Pariente, J. *Chem. Mater.* **2001**, *13*, 308−311.
(11) Lu, J.; Liong, M.; Zink, J. I.; Tamanoi, F. *Small* **2007**, *3*, 1341−1346.
(12) Jo, S. M.; Kim, J. C. *Colloid Polym. Sci.* **2009**, *287*, 1065−1070.
(13) Liu, J. W.; Jiang, X. M.; Ashley, C.; Brinker, C. J. *J. Am. Chem. Soc.* **2009**, *131*, 7567−7569.
(14) Liu, J. W.; Stace-Naughton, A.; Jiang, X. M.; Brinker, C. J. *J. Am. Chem. Soc.* **2009**, *131*, 1354−1355.
(15) Koning, G. A.; Krijger, G. C. *Anti-Cancer Agents Med. Chem.* **2007**, *7*, 425−440.
(16) Pan, J.; Wan, D.; Gong, J. L. *Chem. Commun.* **2011**, *47*, 3442−3444.
(17) Peer, D.; Zhu, P. C.; Carman, C. V.; Lieberman, J.; Shimaoka, M. *Proc. Natl. Acad. Sci. U.S.A.* **2007**, *104*, 4095−4100.
(18) Davis, M. E.; Chen, Z.; Shin, D. M. *Nat. Rev. Drug Discovery* **2008**, *7*, 771−782.
(19) Ashley, C. E.; Carnes, E. C.; Phillips, G. K.; Padilla, D.; Durfee, P. N.; Brown, P. A.; Hanna, T. N.; Liu, J. W.; Phillips, B.; Carter, M. B.; Carroll, N. J.; Jiang, X. M.; Dunphy, D. R.; Willman, C. L.; Petsev, D. N.; Evans, D. G.; Parikh, A. N.; Chackerian, B.; Wharton, W.; Peabody, D. S.; Brinker, C. J. *Nat. Mater.* **2011**, *10*, 389−397.
(20) Xing, Z. M.; Wang, C. L.; Yan, J.; Zhang, L.; Li, L.; Zha, L. S. *Soft Matter* **2011**, *7*, 7992−7997.
(21) Kaiden, T.; Yuba, E.; Harada, A.; Sakanishi, Y.; Kono, K. *Bioconjugate Chem.* **2011**, *22*, 1909−1915.
(22) Zhang, J.; Zhang, M.; Tang, K.; Verpoort, F.; Sun, T. *Small* **2013**, 1−15.
(23) Mashaghi, S.; Jadidi, T.; Koenderink, G.; Mashaghi, A. *Int. J. Mol. Sci.* **2013**, *14*, 4242−4282.
(24) Zhang, X.; Yang, P.; Dai, Y.; Ma, P. a.; Li, X.; Cheng, Z.; Hou, Z.; Kang, X.; Li, C.; Lin, J. *Adv. Funct. Mater.* **2013**, *23*, 4067−4078.
(25) Hu, X.; Hao, X.; Wu, Y.; Zhang, J.; Zhang, X.; Wang, P. C.; Zou, G.; Liang, X.-J. *J. Mater. Chem. B* **2013**, *1*, 1109−1118.
(26) Chen, C.-Y.; Kim, T. H.; Wu, W.-C.; Huang, C.-M.; Wei, H.; Mount, C. W.; Tian, Y.; Jang, S.-H.; Pun, S. H.; Jen, A. K. Y. *Biomaterials* **2013**, *34*, 4501−4509.
(27) Li, Y.; Gao, G. H.; Lee, D. S. *Adv. Healthcare Mater.* **2013**, *2*, 388−417.
(28) Johnson, R. P.; Jeong, Y. I.; John, J. V.; Chung, C. W.; Kang, D. H.; Selvaraj, M.; Suh, H.; Kim, I. *Biomacromolecules* **2013**, *14*, 1434−1443.
(29) Yang, Y.; Song, W. X.; Wang, A. H.; Zhu, P. L.; Fei, J. B.; Li, J. B. *Phys. Chem. Chem. Phys.* **2010**, *12*, 4418−4422.
(30) Liu, J. W.; Stace-Naughton, A.; Brinker, C. J. *Chem. Commun.* **2009**, 5100−5102.
(31) Zhou, W. T.; An, X. Q.; Wang, J. Z.; Shen, W. G.; Chen, Z. Y.; Wang, X. Y. *Colloid Surf. A: Physicochem. Eng. Asp.* **2012**, *395*, 225−232.

(32) Kono, K.; Nakai, R.; Morimoto, K.; Takagishi, T. *Biochim. Biophys. Acta* **1999**, *1416*, 239−250.
(33) Kono, K.; Henmi, A.; Yamashita, H.; Hayashi, H.; Takagishi, T. *J. Controlled Release* **1999**, *59*, 63−75.
(34) Zignani, M.; Drummond, D. C.; Meyer, O.; Hong, K.; Leroux, J. C. *Biochim. Biophys. Acta* **2000**, *1463*, 383−394.
(35) Hafez, I. M.; Cullis, P. R. *Adv. Drug Delivery Rev.* **2001**, *47*, 139−148.
(36) Meyer, O.; Papahadjopoulos, D.; Leroux, J. C. *FEBS Lett.* **1998**, *421*, 61−64.
(37) Hong, M. S.; Lim, S. J.; Oh, Y. K.; Kim, C. K. *J. Pharm. Pharmacol.* **2002**, *54*, 51−58.
(38) Zhao, X. B. B.; Lee, R. J. *Adv. Drug Delivery Rev.* **2004**, *56*, 1193−1204.
(39) Fonseca, C.; Moreira, J. N.; Ciudad, C. J.; de Lima, M. C. P.; Simoes, S. *Eur. J. Pharm. Biopharm.* **2005**, *59*, 359−366.
(40) Simoes, S.; Moreira, J. N.; Fonseca, C.; Duzgunes, N.; de Lima, M. C. P. *Adv. Drug Delivery Rev.* **2004**, *56*, 947−965.
(41) Roux, E.; Francis, M.; Winnik, F. M.; Leroux, J. C. *Int. J. Pharm.* **2002**, *242*, 25−36.
(42) Roux, E.; Lafleur, M.; Lataste, E.; Moreau, P.; Leroux, J. C. *Biomacromolecules* **2003**, *4*, 240−248.
(43) Roux, E.; Stomp, R.; Giasson, S.; Pezolet, M.; Moreau, P.; Leroux, J. C. *J. Pharm. Sci.* **2002**, *91*, 1795−1802.
(44) Klibanovl, A. L.; Maruyamal, K.; Torchilin2, V. P.; Huang, L. *FEBS Lett.* **1990**, *268*, 235−237.
(45) Zhigaltsev, I. V.; Maurer, N.; Wong, K. F.; Cullis, P. R. *Biochim. Biophys. Acta* **2002**, *1565*, 129−135.
(46) Kim, J. C.; Bae, S. K.; Kim, J. D. *J. Biochem.* **1997**, *121*, 15−19.
(47) Sudimack, J. J.; Guo, W. J.; Tjarks, W.; Lee, R. J. *Biochim. Biophys. Acta* **2002**, *1564*, 31−37.
(48) Tang, H. Y.; Guo, J.; Sun, Y.; Chang, B. S.; Ren, Q. G.; Yang, W. L. *Int. J. Pharm.* **2011**, *421*, 388−396.
(49) Datt, A.; El-Maazawi, I.; Larsen, S. C. *J. Phys. Chem. C* **2012**, *116*, 18358−18366.
(50) Bariana, M.; Aw, M. S.; Kurkuri, M.; Losic, D. *Int. J. Pharm.* **2013**, *443*, 230−241.
(51) Rahman, I. A.; Jafarzadeh, M.; Sipaut, C. S. *Ceram. Int.* **2009**, *35*, 1883−1888.
(52) Suwalski, A.; Dabboue, H.; Delalande, A.; Bensamoun, S. F.; Canon, F.; Midoux, P.; Saillant, G.; Klatzmann, D.; Salvetat, J.-P.; Pichon, C. *Biomaterials* **2010**, *31*, 5237−5245.
(53) Cauda, V.; Engelke, H.; Sauer, A.; Arcizet, D.; Brauchle, C.; Radler, J.; Bein, T. *Nano Lett.* **2010**, *10*, 2484−2492.
(54) Cui, Y.; Xu, Q.; Chow, P. K.-H.; Wang, D.; Wang, C.-H. *Biomaterials* **2013**, *34*, 8511−8520.
(55) Wang, D.; Huang, J.; Wang, X.; Yu, Y.; Zhang, H.; Chen, Y.; Liu, J.; Sun, Z.; Zou, H.; Sun, D.; Zhou, G.; Zhang, G.; Lu, Y.; Zhong, Y. *Biomaterials* **2013**, *34*, 7662−7673.
(56) Zheng, J.; Tian, X.; Sun, Y.; Lu, D.; Yang, W. *Int. J. Pharm.* **2013**, *450*, 296−303.
(57) Schmaljohann, D. *Adv. Drug Delivery Rev.* **2006**, *58*, 1655−1670.